lattice constants indicate little mutual solubility between oxide and metal phases.

Samples were cut perpendicular and parallel to the growth direction. Circular specimens with a radius of 8 to 12 mm and 3 to 5 mm thick were examined in the light microscope and, in particular, in the scanning electron microscope (Stereoscan). Specimens were polished, and in some cases a surface layer of UO_2 was etched away (*2*) to expose the tungsten fibers or platelets. For examination in the scanning electron microscope, further preparation (for example, coating with a conductive film) was not needed. The secondary emission mode of the scanning electron microscope was used. The micrograph suggests that tungsten fibers are hexagonal (Fig. 1A). The contrast is due to differences in materials rather than in topography.

The appearance of the sample after it had been etched to expose the tungsten fibers is quite similar to the view one obtains in a light microscope except that the magnification and the depth of focus are significantly increased (Fig. 1B). Emission of secondary electrons from tungsten was much stronger than from UO_2 and makes the tungsten appear in the form of white dots. The fibers are quite well ordered with spacing of fibers ranging from 3 to 6 μm.

The etched fibers in Fig. 1C show well-developed facets, although the pattern of growth may have been altered during etching. The fibers in Fig. 1D are round, and their diameter varies from 0.85 to 1 μm. The different growth forms also imply that several different orientations developed during solidification. Fibers extended the length of the samples studied. Fibers were formed at growth rates of approximately 12 mm/hr. In some isolated areas tungsten solidified in platelets at a growth rate estimated in excess of 20 mm/hr. These platelets were 0.8 to 1 μm thick, extending to more than 50 μm in width and several millimeters in length. A region of less-extensive platelet growth is shown in Fig. 1E.

Orientation relations between metal and oxide were studied in a diffractometer (General Electric, XRD 5) equipped with a goniostat type of single-crystal orienter. The specimens were cut perpendicular to the direction of growth. They consisted of a number of large (several millimeters in diameter) UO_2 grains. Small areas containing predominantly one UO_2–W orientation were examined in a number of specimens. The orientation relation most frequently observed was $(110)_W \parallel (111)_{UO_2}$ (planes perpendicular to growth direction) and with $<110>_W \parallel <110>_{UO_2}$. The indicated parallelism of planes and directions between W and UO_2 denotes only the mutual arrangement of metal and oxide. A number of other less frequently occurring orientation relations were observed as well.

The application of unidirectionally grown refractory oxide-metal composites (cermets) for structures or devices is essentially unexplored. The ordered high-elastic modulus fibers, bonded strongly to the oxide matrix, certainly must enhance the mechanical properties of the oxide. The thermal and electrical behavior of the composite will be very directional.

R. J. GERDES, A. T. CHAPMAN
Georgia Institute of Technology,
Atlanta 30332

G. W. CLARK
Oak Ridge National Laboratory,
Oak Ridge, Tennessee 37831

References

1. A. T. Chapman and G. W. Clark, *J. Amer. Ceram. Soc.* **48**, 495 (1965); ———, D. E. Hendrix, "UO_2–W Cermets Produced by Unidirectional Solidification," 71st Meeting of the American Ceramic Society, Washington, D.C., 1969.
2. A. J. Manly, *J. Nucl. Mater.* **15**, 143 (1965).

29 August 1969; revised 20 October 1969 ■

Water in the Earth's Mantle: Melting Curves of Basalt-Water and Basalt-Water–Carbon Dioxide

Abstract. *At depths below about 45 kilometers in the earth, the presence of high proportions of carbon dioxide does not significantly affect the temperature of the beginning of melting of basalt-water compositions. Water must be present only in trace amounts in the solid part of the silicate mantle if it contains appreciable proportions of basaltic composition.*

The upper mantle of the earth is thought to consist predominantly of peridotite (*1*), which on partial melting, together perhaps with differentiation, yields melts of basaltic composition (*2*). The pervasiveness of basaltic magmas through most of geologic time indicates that at least parts of the mantle have been at temperatures above those of the basalt solidus during most of its thermal history. Experimental determinations of the dry melting of basalt (*3*) and peridotite (*4*) at high pressures place an upper limit on temperatures in the interior of the earth. However, it is now well known that water under pressure greatly lowers the melting temperatures of rock-forming silicates, and previous high-pressure studies on granite (*5*) and basalt (*6*) saturated with water place lower limits on the temperature of melting in the crust and mantle of the earth. Although some of the volatiles present in the primordial earth escaped shortly after accretion (*7*), the compositions of volcanic gases in equilibrium with basalts (*8*) and the concept that the hydrosphere and atmosphere evolve by degassing (*9*) suggest that significant amounts of water are contained within the interior of the earth.

We have succeeded in determining the beginning of melting of a natural tholeiitic basalt (*10*) to pressures of 30 kb in the presence of water and water–carbon dioxide mixtures. We use the term "basalt" to refer to a composition, not a rock type. All experiments were performed in a piston-cylinder apparatus (*11*) using a 2.5-cm sample chamber. The charges were sealed in Ag-Pd capsules (*12*) either with 15 percent of water by weight or 9 to 15 percent oxalic acid, which dissociates and oxidizes to produce a mixture of 50 mole percent each of water and carbon dioxide (71 percent of carbon dioxide by weight) (*13*). Additional experimental details and results have been obtained and are forthcoming (*14*).

Curves representing the beginning of melting and the upper stability limits of plagioclase and amphibole appear in a simplified pressure-temperature projection (Fig. 1). Clinopyroxene, epidote, and quartz are part of the subsolidus assemblages for both compositions above 10 kb pressure. Garnet and clinopyroxene are stable above the amphibole-out curves at pressures above about 15 kb. Note that at high pressures the stability of the hydrous mineral amphibole is increased as the result of the lowering of the activity of water, by the addition of carbon dioxide, as predicted from work in synthetic systems (*15*).

Our vapor-saturated solidus for basalt-water compositions, which is in agreement with that determined for a high-alumina basalt by Lambert and Wyllie (*6*), is at temperatures much below those in the mantle (*16*) (Fig. 1). Therefore, if the equilibrium pressure (*17*) of water (P_{eH_2O}) is nearly equal to total pressure (P_T) in the mantle and if the mantle contains appreciable amounts of basaltic composition, free water in a vapor phase would cause partial melting, generating large proportions of water-saturated liquid. Consequently, a solid silicate mantle requires that P_{eH_2O} be less than P_T, with perhaps most of the water confined in hydrous minerals. The proportions of water in the mantle are undoubtedly much less than those in the experiments used to determine the basalt-water solidus, and the presence of major proportions of carbon dioxide and other components in fluid inclusions in basaltic rocks (*18*) and in volcanic gases (*8*) indicates that P_{eH_2O} is less than P_T. For these reasons, we used the arbitrary vapor composition of about 71 percent of carbon dioxide by weight to determine the solidus for basalt-water–carbon dioxide compositions (Fig. 1). Of course, the temperature of the beginning of melting at any given pressure changes with different ratios of carbon dioxide to water. The abrupt changes in the slopes of the basalt melting curves at about 15 kb pressure results principally from the transition of plagioclase to denser phases, including pyroxene and amphibole (*5, 19*). Similar transformations in the anhydrous system result in much less pronounced inflections (*3*).

At relatively low pressures, the presence of the carbon dioxide raises the temperature of the solidus by more than 100°C. Surprisingly, the effect becomes progressively less at elevated pressures, and above 15 kb the difference is petrogenetically insignificant. This results, in part, from appreciable solubility of carbon dioxide in these silicate liquids at pressures above about 15 kb, compared with the very limited solubility at low pressures (*20*). Thus, as shown by the relative positions of our basalt-water–carbon dioxide solidus and the geothermal gradient (Fig. 1), even large ratios of carbon dioxide to water result in melting in the mantle if the fluid pressure (P_f) is equal or nearly equal to P_T. It is improbable that P_f is much less than P_T in the mantle, because rocks will not support large differential stresses at these high temperatures and pressures for geological time periods.

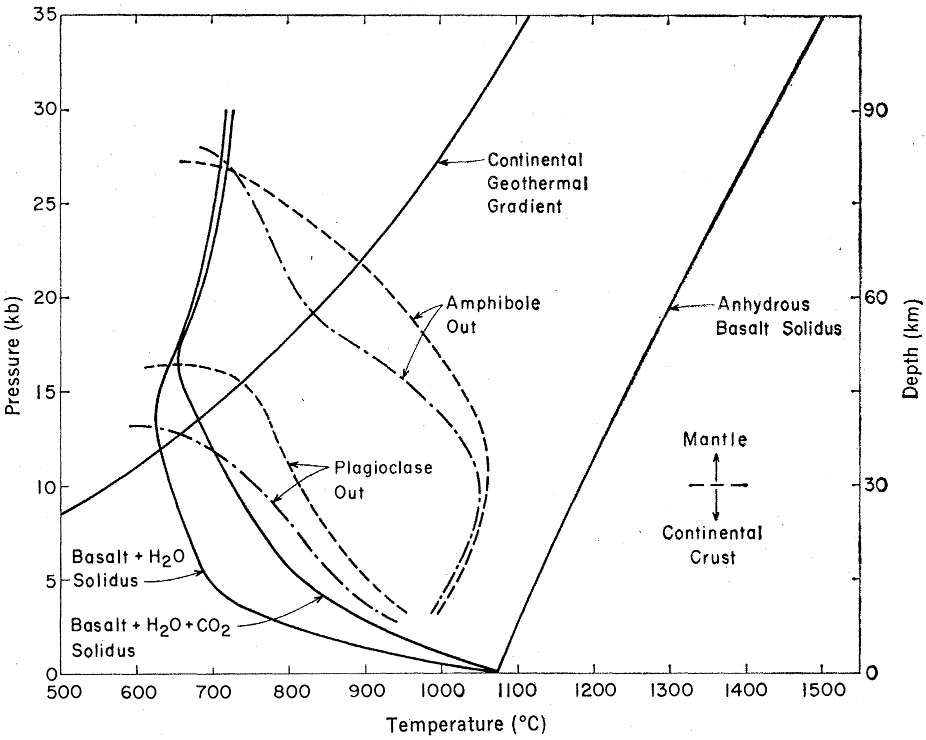

Fig. 1. Pressure-temperature projection of curves representing the beginning of melting of vapor-saturated basalt-water and basalt-water–carbon dioxide compositions, compared with the curves representing the beginning of melting of dry basalt (*3*) and the continental geothermal gradient using a heat flow of 1.5 μcal cm^{-2} sec^{-1} (*16*). The dashed curves for the upper stability of plagioclase and amphibole are for the basalt-water–carbon dioxide compositions; the dash-dot curves refer to the basalt-water compositions. The horizontal dashed line is the average depth of the continental Moho. The phase relationships for basalt-water–carbon dioxide at 2 and 5 kb are based on the results by Holloway (*24*).

The maximum proportion of hydrous minerals (amphiboles) in our experiments is about 50 percent by weight, which indicates that about 1.0 percent or less, by weight, of the total charge is combined water. Even if it is assumed that all such combined water is unavailable for magma generation (*6, 21*), amounts greater than this value would result in melting if the upper mantle is basaltic in composition; the solidus for more magnesian peridotitic compositions may be at higher temperatures. For example, one experiment at 775°C and 15 kb with 2.7 percent of water by weight and 6.3 percent carbon dioxide resulted in about 5 percent liquid, even though some water was bound in amphibole. At pressures above 25 kb, at the temperatures of the melting curves for basalt-water and basalt-water–carbon dioxide, and at yet lower pressures at higher temperatures, our experiments indicate that amphiboles are unstable, as postulated by Lambert and Wyllie (*6*), and essentially all water would be dissolved in silicate liquids.

Therefore, a solid silicate mantle requires that water not be present in appreciable amounts as a free vapor phase, even with weight ratios of carbon dioxide to water as high as 2.5. The low-velocity zone in the upper mantle (*22*) may be explained as one where incipient melting attenuates seismic waves (*23*), as suggested by the intersection of the geothermal gradient and the melting curves (Fig. 1). However, the large proportions of liquid in the present experiments at temperatures near those on the geothermal gradient above 15 kb pressure indicate that water in the mantle, although certainly present, must occur predominantly in hydrous minerals or in equivalent amounts under conditions where such minerals are unstable. It is probable that the proportion of hydrous minerals in the peridotite of the upper mantle is less than that in our experiments, requiring that water be present in amounts much less than 1.0 percent.

ROBIN E. T. HILL, A. L. BOETTCHER
Department of Geochemistry and Mineralogy, Deike Building, Pennsylvania State University, University Park 16802

References and Notes

1. A. E. Ringwood, *J. Geophys. Res.* **67**, 857 (1962); F. Birch, in *The Earth's Crust and Upper Mantle*, P. J. Hart, Ed. (American Geophysical Union, Washington, D.C., 1969), p. 18.
2. D. H. Green and A. E. Ringwood, *Contrib. Mineral. Petrology* **15**, 103 (1967); M. J. O'Hara, *Earth-Sci. Rev.* **4**, 69 (1968).
3. L. H. Cohen, K. Ito, G. C. Kennedy, *Amer. J. Sci.* **265**, 475 (1967).
4. K. Ito and G. C. Kennedy, *ibid.*, p. 519; I. Kushiro, Y. Syono, S. Akimoto, *J. Geophys. Res.* **73**, 6023 (1968).
5. A. L. Boettcher and P. J. Wyllie, *J. Geol.* **76**, 235 (1968).
6. I. B. Lambert and P. J. Wyllie, *Nature* **219**, 1240 (1968).
7. A. E. Ringwood, *Geochim. Cosmochim. Acta* **30**, 41 (1966).
8. B. E. Nordlie, *Geol. Soc. Amer. Spec. Pap.* **115**, 166 (1968).
9. W. W. Rubey, in *Crust of the Earth*, A. Poldervaart, Ed. (Geological Society of America, New York, 1955), p. 631; H. Holland, in *Petrologic Studies*, A. E. J. Engel, H. L. James, B. F. Leonard, Eds. (Geological Society of America, New York, 1962), p. 447.
10. Similar to the olivine tholeiite, 1921 flow of Kilauea, Hawaii, listed as No. 14, Table 2, by H. S. Yoder, Jr., and C. E. Tilley, *J. Petrol.* **3**, 342 (1962).
11. F. R. Boyd and J. L. England, *J. Geophys. Res.* **65**, 741 (1960).
12. A. Muan, *Amer. Ceram. Soc. Bull.* **42**, 344 (1963).
13. J. R. Holloway, C. Wayne Burnham, G. L. Millhollen, *J. Geophys. Res.* **73**, 6598 (1968).
14. R. E. T. Hill and A. L. Boettcher, in preparation.
15. A. L. Boettcher, *Trans. Amer. Geophys. Union* **50**, 352 (1969); H. S. Yoder, Jr., and I. Kushiro, *Amer. J. Sci.* **267-A**, 558 (1969).
16. S. P. Clark, Jr., and A. E. Ringwood, *Rev. Geophys.* **2**, 35 (1964).
17. H. J. Greenwood, *J. Geophys. Res.* **66**, 3923 (1961).
18. E. Roedder, *Amer. Mineral.* **50**, 1746 (1965).
19. A. L. Boettcher and P. J. Wyllie, *Amer. J. Sci.* **267**, 875 (1969); *Nature* **216**, 572 (1967).
20. P. J. Wyllie and O. F. Tuttle, *Amer. J. Sci.* **257**, 648 (1959).
21. C. Wayne Burnham, in *Geochemistry of Hydrothermal Ore Deposits*, H. L. Barnes, Ed. (Holt, Rinehart & Winston, New York, 1967), p. 34.
22. F. Press, *Science* **165**, 174 (1969).
23. H. Spetzler and D. L. Anderson, *J. Geophys. Res.* **73**, 6051 (1968).
24. J. R. Holloway, private communication.

25. We thank C. Wayne Burnham for helpful discussion and for reviewing the manuscript. R. Z. Small and Miss Tony Gardner assisted us in the laboratory. This work was supported by grant GA-1364 from the National Science Foundation.

21 November 1969; revised 15 December 1969 ■

Magnetic Particles Extracted from Manganese Nodules: Suggested Origin from Stony and Iron Meteorites

Abstract. *On the basis of x-ray diffraction and electron microprobe data, spherical and ellipsoidal particles extracted from manganese nodules were divided into three groups. Group I particles are believed to be derived from iron meteorites, and Group II particles from stony meteorites. Group III particles are believed to be volcanic in origin.*

Cosmic spherules in manganese nodules were first recognized by Murray and Renard (*1*), but no detailed study of their characteristics has been published. Since manganese nodules apparently grow more slowly than deep sea sediments are deposited (*2*), it appeared possible to obtain significant numbers of spherules from relatively small amounts of material, unbiased by the addition of recent industrial contaminants.

Twenty-one manganese nodules and manganese oxide crusts from various oceanographic stations were crushed, and the magnetic fraction was removed with a hand magnet covered with cellophane. Fifty-five spherical and ellipsoidal particles were handpicked from the magnetic fractions under a binocular microscope.

The mean concentration of the magnetic spherules in manganese nodules is about 400 spherules (>100 μm in diameter) per kilogram of sample and ranges from 0 to about 3500 per kilogram. This concentration is higher than the concentration of spherules in deep sea sediments ($330 > 30$ μm/kg) (*3*), salt deposits ($4 > 25$ μm/kg) (*4*), and beach sands ($6 > 180$ μm/kg) (*5*).

Nineteen spherules were analyzed by x-ray diffraction (powder and precession cameras) and electron microprobe techniques. The spherules were divided into four categories (Table 1). Ten of the 19 spherules (Group I) are black, shiny, spherical, and commonly have a depression or dimple on the surface. Each spherule consists of an oxide phase of magnetite and wüstite, both containing 1 to 4 percent nickel, commonly surrounding an acentric, metallic nucleus containing about 50 to 75 percent nickel (Fig. 1). Precession photographs show that the magnetite, which usually forms an outer shell, is a homogeneous single crystal. The wüstite phase, visible in Fig. 1 as an inner shell, is probably a single crystal since it gives a spotty powder photograph, as does the magnetite; however, it was not positively identified in the precession photographs. The metallic core is polycrystalline.

The three Group II spherules are also black, shiny, and spherical, but without dimples. Precession photographs show that they consist of multicrystalline aggregates of magnetite and wüstite with nearly parallel orientations. In one particle (Albatross 13, No. 2), the oxide phase surrounds a nickel-rich metallic nucleus. The oxide phase of Group II particles is transected by a rectangular network of lamellas containing major iron and subordinate silicon and lesser amounts of magnesium, aluminum, and calcium (Fig. 2).

The internal structure and preferred crystallographic orientation of Group II spherules suggests that the oxide phase was formed by dendritic growth, and thus the silicate phase was confined to the interdendritic area. The absence of a diffraction pattern from the silicate phase may be due to its

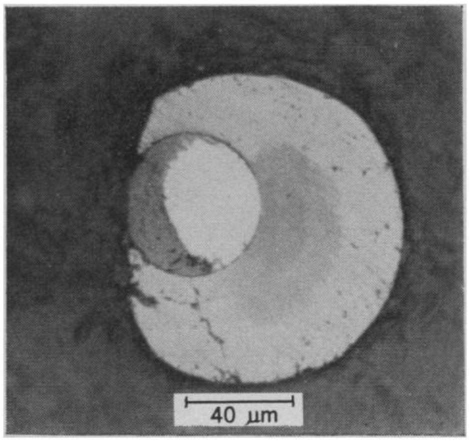

Fig. 1. Challenger 276, No. 1. This Group I particle shows a magnetite (light-gray) outer shell, wüstite (medium-gray) inner shell, and a metallic nucleus (white), which is partly oxidized to trevorite (dark gray).

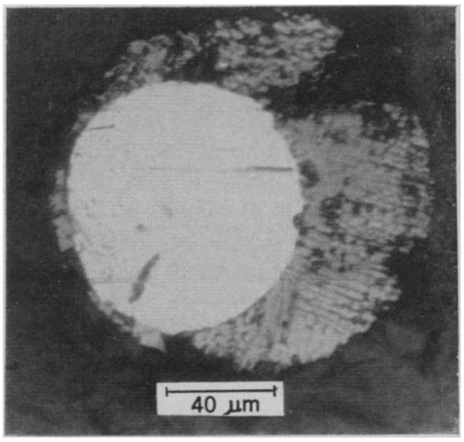

Fig. 2. Albatross 13, No. 2. This Group II particle shows an oxide shell (gray) and silicon-rich lamellas (dark gray), which surround a large metallic nucleus (white).